Hydrology and Earth System Sciences, 2(2–3), *265–281* (1998) © EGS

Hydrology & Earth System Sciences

A grid-based distributed flood forecasting model for use with weather radar data: Part 1. Formulation

V.A. Bell and R.J. Moore

Institute of Hydrology, Wallingford, Oxfordshire, OX10 8BB, UK

Abstract

A practical methodology for distributed rainfall-runoff modelling using grid square weather radar data is developed for use in real-time flood forecasting. The model, called the Grid Model, is configured so as to share the same grid as used by the weather radar, thereby exploiting the distributed rainfall estimates to the full. Each grid square in the catchment is conceptualised as a storage which receives water as precipitation and generates water by overflow and drainage. This water is routed across the catchment using isochrone pathways. These are derived from a digital terrain model assuming two fixed velocities of travel for land and river pathways which are regarded as model parameters to be optimised. Translation of water between isochrones is achieved using a discrete kinematic routing procedure, parameterised through a single dimensionless wave speed parameter, which advects the water and incorporates diffusion effects through the discrete space-time formulation. The basic model routes overflow and drainage separately through a parallel system of kinematic routing reaches, characterised by different wave speeds but using the same isochrone-based space discretisation; these represent fast and slow pathways to the basin outlet, respectively. A variant allows the slow pathway to have separate isochrones calculated using Darcy velocities controlled by the hydraulic gradient as estimated by the local gradient of the terrain. Runoff production within a grid square is controlled by its absorption capacity which is parameterised through a simple linkage function to the mean gradient in the square, as calculated from digital terrain data. This allows absorption capacity to be specified differently for every grid square in the catchment through the use of only two regional parameters and a DTM measurement of mean gradient for each square. An extension of this basic idea to consider the distribution of gradient within the square leads analytically to a Pareto distribution of absorption capacity, given a power distribution of gradient within the square. The probability-distributed model theory (Moore, 1985) can then be used directly to obtain the integrated runoff production for the square for routing to the catchment outlet. Justification for the simple linkage function is in part sought through consideration of variants on the basic model where (i) runoff production is based on a topographic index control on saturation and (ii) absorption capacity is related to the Integrated Air Capacity of the soil, as obtained from soil survey. An impervious area fraction is also introduced based on the use of Landsat classified urban areas. The Grid Model and its variants are assessed in Part 2 (Bell and Moore, 1998), first as simulation models and then as forecasting models, following the development of updating procedures to accommodate recent observations of flow so as to improve forecast performance in a real-time context.

Introduction

Starting from the viewpoint of simple, conceptual models rather than physically-based models, the traditional approach to modelling the response of a river basin to rainfall is through a lumped representation in which an estimate of catchment average rainfall is used as input. This persists as the most commonly employed approach, particularly for real-time flood forecasting applications. In such applications it is common to require only a forecast at a 'basin outlet' location which is gauged and there is less interest in forecasts at internal locations or a form of model parameterisation capable of predicting the effect of land-use change. Experience has shown that, with adequate calibration data in the form of flow records and with only sparse sampling of the rainfall field using raingauges, more complex, and possibly more realistic, distributed models fail to provide improved forecast accuracy. A common diagnosis is that the models are 'input limited' and that improved performance from distributed models will only be achieved when better measurements of rainfall fields are used as input data (O'Connell and Clarke, 1981; Todini, 1988). Such measurements are now increasingly available in the form of weather radar data, commonly available on a 2 km grid at 5 minute intervals (Collier, 1996).

An intrinsic problem associated with distributed models configured on a square grid is the potentially large number of model parameters which can be involved. If a different set of parameters is used for each grid square, the

total number of parameters can become large even for basins of modest size and there may be strong dependencies between sets. In the Grid Model this problem of 'over-parameterisation' is circumvented through the use of measurements from a digital terrain model (DTM) of the basin together with simple linkage functions. These functions allow many grid-scale model parameters to be prescribed through a small number of regional parameters which can be optimised to obtain a good model fit.

The Grid Model has been developed with the aim of formulating a simple distributed rainfall-runoff model suitable for use in real-time flow forecasting with weather radar providing the source of rainfall input. Whilst it is neither natural nor essential to configure such a model on the radar grid, it is the approach which is adopted here. Such an approach is by no means new: an early example is provided by Anderl *et al.* (1976). The approach developed here was first outlined by Moore (1991) with preliminary results given by Moore (1992), Moore and Bell (1994, 1996) and Moore *et al.* (1994). Other workers have pursued similar lines, but with different structures for the model at a detailed level, most notably Chander and Fattorelli (1991). Polarski (1992) provides a good review of simple distributed conceptual rainfall-runoff models for use with digital terrain data, but not specifically for use with weather radar data.

The structure of the basic form of Grid Model is outlined in the next section. Several model variants are then introduced, including a probability-distributed storage capacity formulation (Moore, 1985) and a topographic index approach to soil moisture distribution (Beven and Kirkby, 1979). Other variants link the storage capacity to the Integrated Air Capacity (IAC) of the soil layer (Hollis and Woods, 1989), extracted from soil survey data, and to Landsat delineated urban areas. Later sections describe how a digital terrain model is used to reduce the number of parameters required to be optimised. A review of the parameters involved in the various model variants is followed by a summary and concluding remarks. An assessment of the basic Grid Model and its variants using data from a range of catchments forms the subject of Part 2, presented as a companion paper (Bell and Moore, 1998).

Part 1 focuses on the formulation of the Grid Model as a simulation model, transforming rainfall (and potential evaporation) to runoff. Experience indicates that the real-time performance of a model, particularly for higher lead times, is influenced by the adequacy of the 'process model' and that updating of the model using recent flow measurements will never fully compensate for an inadequate process description. A simulation model of the rainfall-runoff process suitable for real-time use should be relatively simple, capture the dominant modes of behaviour of the catchment response to rainfall and, ideally, have a structure that is amenable to correction of its state variables, such as the water contents of different conceptual storage elements. Simplicity should encapsulate requirements for ease of initialisation and for a small number of model parameters that are identifiable and have a conceptual meaning that is readily understood. These requirements underpin the form of model developed here. The issue of state correction of the model, and other forms of forecast updating, are considered in Part 2 whilst here the main aim is to set down a suitable simulation model for forecasting purposes.

A distributed formulation is considered in order to make maximum use of information contained in grid square radar data and to allow for incorporating terrain-based information on how runoff production might vary within a catchment. A key question is whether a distributed model offers any improvement for forecasting purposes over and above that obtained from a lumped model. Distributed weather radar may be used to obtain an improved estimate of catchment average rainfall for use in both lumped and distributed model formulations, and the latter may prove superior on account of its better representation of the distributed nature of the catchment response, even for uniform rainfall. If spatial variability of rainfall is dominant, and the nature of the catchment response is sensitive to it, then a distributed model formulation might prove superior. Which approach proves best is likely to depend on storm and catchment characteristics including the effects of scale, the adequacy of the lumped and distributed model formulations and, in particular, the quality of the weather radar estimates of the spatial rainfall fields as compared to point raingauge estimates. These questions and issues provide the motivation for the model assessments described in Part 2 which includes comparison of the Grid Model and its variants with a lumped rainfall-runoff model used operationally for flood forecasting in the UK.

Basic model structure

INTRODUCTION

In order to fully exploit the distributed nature of radar data, the distributed model is configured so as to share the same grid as that used by the weather radar. Each radar grid square is conceptualised in the catchment as a storage mechanism which receives water in the form of precipitation and loses water via overflow ('direct runoff'), evaporation and drainage. The storage mechanism used in the basic form of model is a simple store (tank or bucket) having a finite capacity S_{max}. This capacity can be thought of as an absorption capacity of the grid encompassing surface detention, soil moisture storage and the interception capacity of vegetation and other forms of land use. A fundamental idea used in the basic form of model is that absorption capacity is controlled by the average gradient, $\bar{g}$, of the topography in the grid square which can be calculated readily from a digital terrain model (DTM). This

is clearly a gross approximation but provides a simple paradigm from which to develop a distributed model with links to DTM data. It implies that runoff is more readily generated from steep slopes than shallow ones whilst leaving the particular reasons unspecified. Reasons for steep slopes generating runoff more readily might include thin soils, sparse vegetation, limited opportunity for surface detention and encouragement of downslope drainage. The simple linear function linking absorption capacity to gradient also allows the model to be developed to accommodate a distribution of gradient within a square. It is shown later that for a power distribution of gradient it follows analytically that the distribution of capacity is of Pareto form and that the probability-distributed model theory (Moore, 1985) can be applied directly to obtain a simple expression for the integrated runoff from a grid square.

WATER BALANCE IN A GRID SQUARE

Specifically, for a given grid square, the following linkage function is used to relate the maximum storage capacity, S_{max}, and the average gradient, $\bar{g}$, within a grid square:

$$S_{max} = \left(1 - \frac{\bar{g}}{g_{max}}\right) c_{max}, \qquad (1)$$

for $\bar{g}$ " g_{max}. The parameters g_{max} and c_{max} are upper limits of gradient and storage capacity respectively and act as 'regional parameters' for the catchment model. A measurement of the mean gradient within each grid square of the catchment is obtained from the DTM (although a contour map could be used). Values of S_{max} for all grid squares are determined using only the two model parameters, g_{max} and c_{max}, together with measurements of $\bar{g}$ for each square. The regional parameter g_{max} will be somewhat greater in value than the maximum of the average gradient for each square in the catchment obtained from the DTM; also c_{max} will be greater than the maximum of the S_{max} grid values for the catchment. This allows the square with the highest mean gradient to have a storage capacity greater than zero.

Whilst the validity of Eqn. (1) is readily questioned, both in terms of its linear form and that only one factor - gradient—controls storage capacity, it does provide a simple starting point to develop a distributed model with links to DTM data. Its simplicity also allows for further developments which are analytically tractable to accommodate distributions of gradient and storage capacity within a grid square, and their effect on runoff production. The framework for model development presented here, based on simple linkage functions to topographic data, clearly provides further research opportunities through the exploration of alternative linkage functions which might be thought to be more hydrologically accountable. Other possibilities for representing runoff production within the Grid Model are considered later as competing model variants which are assessed in Part 2. Their inclusion in part serves to empirically justify (or not) the use of Eqn. (1) as the basis of a model formulation giving better forecast performance relative to other possible approaches. We now turn to complete the water balance of a grid square storage.

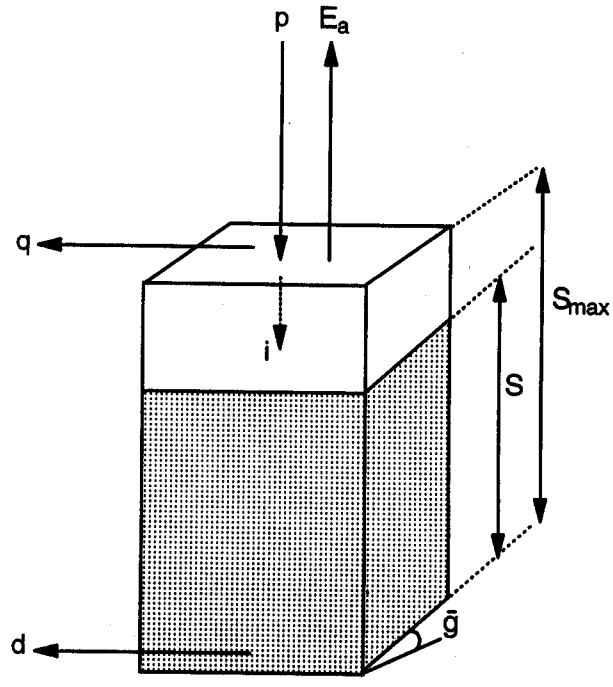

Fig. 1. *A typical grid storage illustrating the components of the water balance.*

A grid storage loses water in three possible ways. If the storage is fully saturated from previous rainfall then any net addition of water spills over and contributes as 'direct runoff' to the fast catchment response. Drainage from the base of the store is controlled by the volume of water in store and contributes to the slow catchment response. Thirdly, water is lost via evaporation to the atmosphere. Figure 1 illustrates a typical grid storage and the components of the water balance involved.

Specifically, a water balance is maintained as follows for each grid square and time interval of duration Δt. (Time and space subscripts are omitted for notational simplicity.) Evaporation loss occurs at the rate, E_a, which is related to the potential evaporation rate, E, and the water in store, S, through the relation

$$E_a = \begin{cases} \left(1 - \dfrac{D - D^*}{S_{\max} - D^*}\right) E, & D \le D^* \\ E, & D > D^*. \end{cases} \quad (2)$$

Here, $D = S_{\max} - S$ is the storage deficit and D^* is the threshold deficit below which evaporation occurs at the potential rate. The value of D^* is common across grid squares.

Drainage from the grid storage, which contributes to the slow catchment response, occurs at the rate

$$d = \begin{cases} k_d S^{\beta}, & S > 0 \\ 0, & otherwise \end{cases} \quad (3)$$

where k_d is the drainage storage constant and the drainage exponent β is a parameter (set here to 3).

A potential infiltration rate is given by

$$i_p = \left(1 - \frac{S}{S_{\max}}\right)^b i_{\max} \quad (4)$$

where $i_{\max}$ is the upper limit of infiltration rate and S is the water in storage. The actual infiltration rate is then given by

$$i = \min(p, i_p) \quad (5)$$

where p is the rainfall rate. Direct runoff generated by this infiltration excess mechanism is simply $q = p - i$. Other infiltration mechanisms could be substituted for the above, which is presented here largely for the sake of completeness. In practice i is set equal to p for modelling the humid temperate basins used in the applications, described in Part 2 (Bell and Moore, 1998), where saturation excess is the dominant runoff mechanism.

Finally, the updated water storage is given by

$$S = \max(0, S + i\Delta t - E_a\Delta t - d\Delta t) \quad (6)$$

and the direct runoff rate contributing to the fast basin response is calculated as

$$q = \max(0, S - S_{\max}) + p\Delta t - i\Delta t). \quad (7)$$

ISOCHRONE-BASED KINEMATIC ROUTING SCHEME

Overview

Direct runoff and drainage generated as outputs from each grid square storage are routed separately to the catchment outlet along a parallel system of fast and slow response pathways, respectively. The spatial mapping of these pathways, and their relationship to the model grid squares, is defined by a single set of isochrones derived from the Digital Terrain Model. Construction of isochrones—lines joining points of equal time of travel to the basin outlet—is achieved initially by assuming that water travels by advection with only two velocities depending on whether the pathway involves land or a river channel (here defined as a blue line on a 1:50000 Ordnance Survey map). In this way it is relatively easy to construct isochrones by direct inference from the distance of a point to the basin outlet and the nature of the pathways involved. (Further details of the construction of isochrones from the Digital Terrain Model are presented later.) Each isochrone band is represented by a routing reach receiving lateral inflows from grid squares within the band. The set of isochrones defines a cascade of routing reaches from the headwaters to the catchment outlet. Each reach is represented by a discrete kinematic wave routing procedure. This not only advects water between the reaches but also incorporates a diffusive component seen in observed hydrographs; in this sense it is not kinematic but, through its discrete space-time formulation, provides an approximation to the convection-diffusion equation. A single parameter, the dimensionless wave speed, characterises the cascade of routing reaches and controls both the advection and attenuation of the flood wave. The fast and slow routing pathways are represented by separate routing cascades characterised by different values for the wave speed parameter; however, they share the same spatial discretisation defined by the isochrone bands. A variant, discussed later, allows for a separate set of slow response isochrones derived from Darcy velocities calculated from the path lengths and gradients obtained from the DTM. The steps which led to this routing scheme are described below together with further details of the routing model formulation.

Isochrone routing scheme

Figure 2 shows an idealised catchment with isochrones overlaid onto the grid squares. From the diagram it can be seen that if $A_{\tau j}$ is the area of grid square j that lies in the catchment between isochrones $\tau - 1$ and τ, then the sum of $A_{\tau j}$ over all m grid squares in the catchment is equal to the area between isochrones $\tau - 1$ and τ in the catchment: that is, $A_\tau = \Sigma_{j=1}^{m} A_{\tau j}$ where $\tau = 1,2,...,n$. Similarly, the area of the jth grid square that lies in the catchment is given by $A_j = \Sigma_{\tau=1}^{n} A_{\tau j}$, $j = 1,2,...,m$, and the total area of the catchment is $A = \Sigma_{\tau=1}^{n} A_\tau = \Sigma_{j=1}^{m} A_j$. Water storage accounting for any grid only partially inside the catchment is treated in the normal way and an adjustment is made when accumulating the direct runoff and drainage across the catchment. Hence, the water input to isochrone τ at time t is

$$I_\tau(t) = \sum_{j=1}^{m} u_{\tau j} r_{tj}, \quad (8)$$

where $u_{\tau j} = A_{\tau j}/A$, and r_{tj} is the grid square outflow rate. The latter can be the direct runoff rate, q_{tj}, or the drainage rate, d_{tj}, depending on whether the model is being used to represent the fast or slow pathway to the basin outlet.

Formally, convolution of the grid square outflow rate per unit area over a grid square, r_{tj}, from grid squares j = 1,2,...,m, to obtain the basin runoff rate per unit area over the basin, Q_t, at time t may be achieved using

$$Q_t = \sum_{j=1}^{m} \sum_{\tau=1}^{n} u_{\tau j} r_{(t-\tau)j} = \sum_{\tau=1}^{n} I_\tau(t - \tau). \quad (9)$$

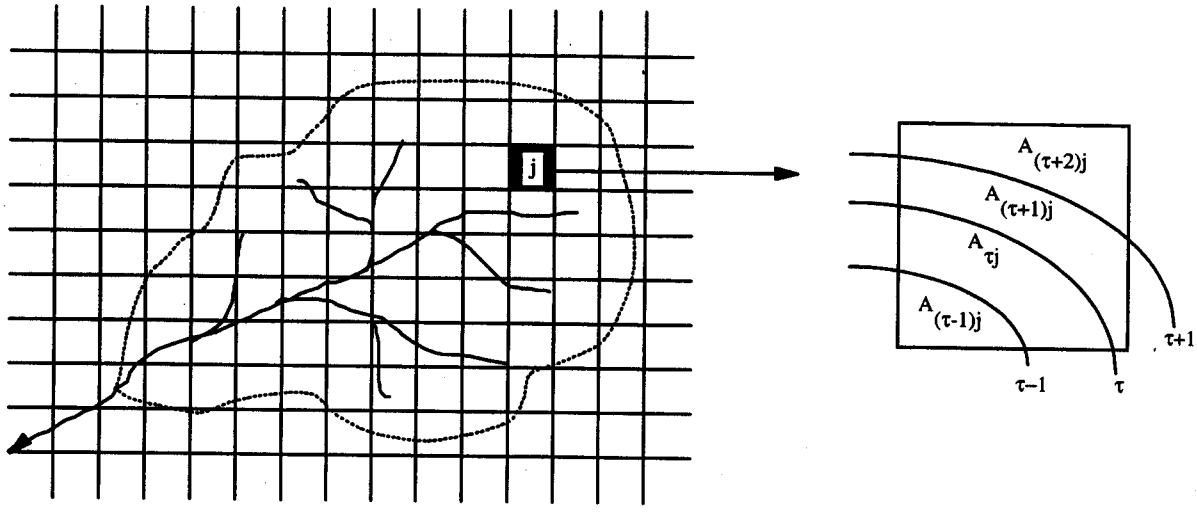

Fig. 2. *Catchment with superimposed weather radar grid and inset showing isochrones in grid square j.*

This routing formulation can be interpreted as a distributed form of unit hydrograph. For uniform direct runoff (effective rainfall in a UH context) over the basin, the underlying classical unit hydrograph is obtained as $v_\tau = A_\tau/A$, $\tau = 1,2,...,n$, with catchment runoff given by the convolution $\sum_{\tau=1}^{n} v_\tau r_{(t-\tau)}$. The relation between $u_{\tau j}$ and v_τ is $u_{\tau j} = w_{\tau j} v_j$ where $w_{\tau j} = A_{\tau j}/A_\tau$. The next section identifies weaknesses in this formulation leading to the adoption of the discrete kinematic wave routing scheme.

Discrete kinematic wave routing scheme

Early versions of the model were based on the distributed unit-hydrograph formulation of Eqn. (9). Initial trials revealed two weaknesses: the first was the computer time involved in computing the discrete form of convolution integral, particularly as part of a parameter optimisation process. The second weakness was the pure form of advection routing implied by the use of the isochrone method and the need to introduce a diffusive element to obtain the more attenuated catchment response seen in practice.

A simple way of introducing diffusion into the isochrone formulation is to assume that each isochrone strip, instead of operating as a simple advection time delay, can be represented by a discrete kinematic wave. Specifically, the idea is to replace the n isochrone strips by a cascade of n reaches, with the outflow from the kth reach at time t represented by

$$q_t^k = (1-\theta)q_{t-1}^k + \theta(q_{t-1}^{k+1} + r_t^k). \qquad (10)$$

Here, r_t^k is the outflow rate from the kth isochrone strip calculated for the interval $(t-1, t)$ and serves as the lateral inflow to the kth reach. Parameter θ is a dimensionless wave speed taking values in the range 0 to 1. The flow rate q_t^1 corresponds to the total outflow from the catchment. Moore and Jones (1978) show how this formulation may be derived from either a discrete form of the kinematic wave equation or a linear storage form of routing. The parameter θ is related to the kinematic wave speed, c, through $\theta = c\Delta t/\Delta x$ where Δt and Δx are the time and space intervals of the discretisation. For a reach of length L sub-divided into N reaches of equal length, $\Delta x = L/N$, then a condition for stability is $\theta < 1$ or $c < L/(N\Delta t)$.

A feature of the routing model is that a single parameter, θ, the dimensionless wave speed controls both the speed and attenuation of the flood wave. This is regarded here as an advantage in providing a parsimonious model parameterisation. Note that the space step also controls these two quantities and this varies from reach to reach as defined by the isochrone spacing, which in turn is controlled by the path length and velocities used in the construction of the set of isochrones. The model does not allow for the wave speed to vary with discharge although such an extension is possible.

As previously mentioned, r_t^k is used as a generic term for 'lateral inflow' generated from grid squares within isochrone band k: in the present context it relates to direct runoff or drainage depending on whether the routing model is used to represent the fast or slow pathway to the catchment outlet. The approach adopted in the main form of the Grid Model routes direct runoff and drainage separately using two parallel discrete kinematic wave models, characterised by different wave speeds θ_s and θ_b respectively, but sharing the same spatial discretisation defined by the set of isochrones. This routing formulation has been adopted for use in the basic Grid Model and in the model variants described next. A schematic depicting the overall structure of the basic Grid Model incorporating the parallel system of routing cascades is shown in Fig. 3. This model is referred to as the Simple Grid Model or SGM. The simple schematic shows four isochrone bands and their mapping onto four-reach routing cascades; the kth

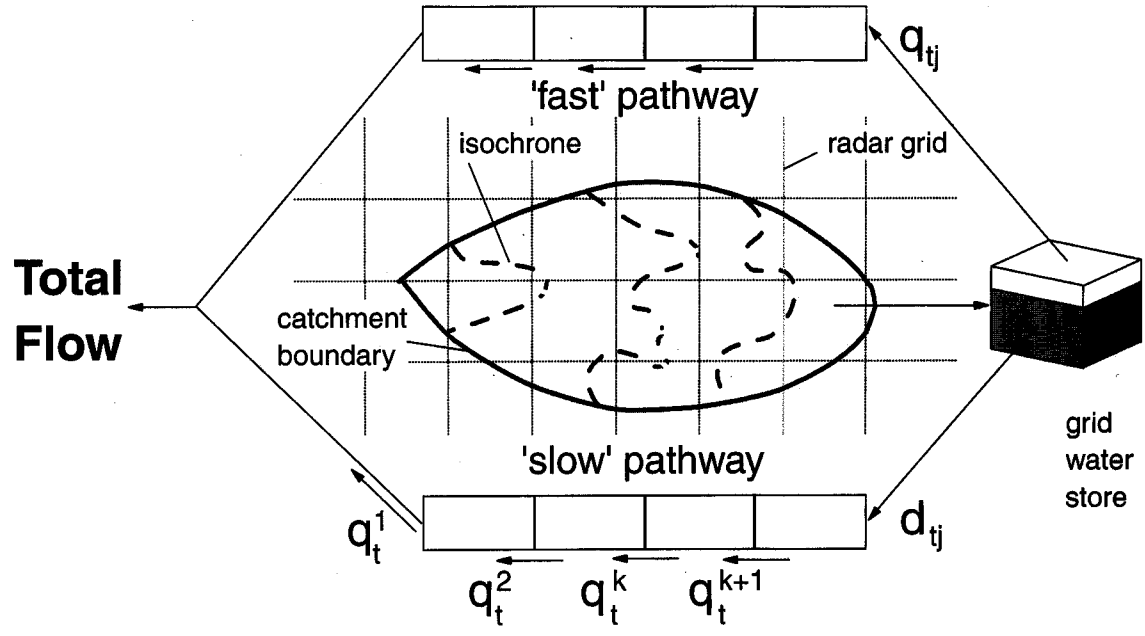

Fig. 3. *The Simple Grid Model.*

reach corresponding to the notation in Eqn. (10) is presented here for $k = 3$.

Variants on the basic Grid Model

The simplicity of the basic Grid Model structure permits the incorporation, and investigation of, a number of model variants. The first three variants introduced here are used to investigate whether the representation of spatial variability within a grid square leads to improved model performance. The simple linkage between storage capacity and mean gradient within a grid square is first extended to four quartile classes of gradient within a grid square. It is then further extended to a probability-distributed representation of gradient within a square which, through the linkage function, is used to derive a distribution of storage capacity for a square. Thirdly, a topographic index formulation of soil saturation is introduced into the Grid Model as an alternative method of calculating the proportion of the grid square that is saturated and generating surface runoff. Also, integrated air capacity data obtained from soil surveys is included in a further model variant by relating these data to storage capacity. A final variant makes use of Landsat classifications of urban area to identify the fraction of a grid that can be considered to have zero storage capacity.

GRADIENT QUARTILE DISTRIBUTED STORAGE FORMULATION

The storage capacity of each grid square in the basic Grid Model is related to the average gradient. With the grid square being chosen to be coincident with a radar grid square, and with the UK having a 2 km radar grid and a 50 m DTM, there will be 400 DTM elevations from which to calculate gradients within each quartile class. As an initial exploration of the value of introducing greater within-grid variability within the model, each square has been sub-divided into four classes based on gradient quartiles. The quartile values of gradient and the average gradients within each quartile class are calculated and used in Eqn. (1) to obtain the corresponding storage capacities for each of the four classes, which by definition have equal area but in general are not made up of contiguous constituents. In other respects the Grid Model essentially operates as before. Generalisation from four to any number of internal gradient classes, and consequently more stores per grid square, is clearly possible but at the cost of increased model run times. It should be noted that this approach corresponds to approximating the continuous probability density function (pdf) of gradient over a grid square by a discrete function. An alternative would be to use a parametric form of pdf and develop analytical solutions for the runoff generated from a grid, following the approach of Moore (1985). The result can be very efficient computationally, relative to the discrete approximation approach, depending on the parametric function adopted. However, the simple discrete approximation approach provides an initial means of exploring whether a more distributed representation is likely to be of benefit. The parametric approach is developed in the next subsection.

PROBABILITY-DISTRIBUTED STORAGE FORMULATION

In this formulation the simple empirical relation between gradient, g, and storage capacity, c, at a point

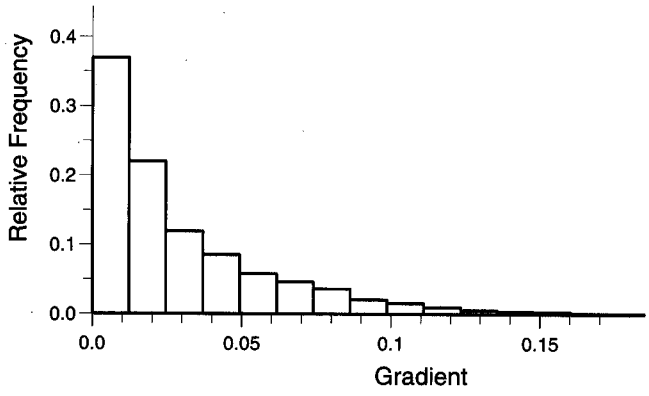

Fig. 4. *Frequency histogram of gradient obtained from DTM data for the Mole catchment.*

$$c = (1 - g / g_{max})c_{max}, \quad (11)$$

where g_{max} and c_{max} are the regional maxima gradient and storage capacity parameters, is used to develop a probability-distributed storage capacity formulation as an extension to the approach presented by Moore (1985). For a given distribution of gradient within a grid square, Eqn. (11) can be used to derive the distribution of storage capacity over the square in terms of the parameters defining the distribution of gradient.

The choice of distribution can be guided by constructing frequency histograms of gradient from DTM data, both for within-grid square areas and for the whole catchment. An example histogram is shown in Fig. 4 for the Mole to Kinnersley Manor catchment in the Thames Basin of the UK. A particular distribution can be fitted to the frequency histogram of gradient and the distribution parameters then used in the derived distribution for storage capacity. The probability-distributed model theory presented by Moore (1985) can then be employed to obtain the proportion of each grid square which is saturated and in turn the volume of runoff generated.

Central to this modelling approach, here applied to a grid square, is the unique relationship that exists between the total water in storage, $S(t)$, and the critical capacity, $C^*(t)$, below which all stores are full, from which the volume of total runoff production, $V(t)$ can be calculated. Specifically, the total water in storage over the grid square is

$$S(t) = \int_0^{C^*(t)} (1 - F(c))dc, \quad (12)$$

where the function $F(.)$ is the distribution function of storage capacity. For a given value of total water in storage, S(t), this can be used to obtain $C^*(t)$ which allows the volume of direct runoff from the square, $V(t + \Delta t)$, to be calculated from

$$V(t + \Delta t) = \int_{C^*(t)}^{C^*(t+\Delta t)} F(c)dc. \quad (13)$$

An overall distribution function for the catchment storage capacity is derived and applied to each grid square by calculating the appropriate distribution parameter for each square from information derived from the DTM. The derivation of the distribution function for a power function of gradient now follows.

Power function distribution of gradient

Consider gradients in the range $0 \leq g \leq g_{max}$ which follow a power distribution of the form

$$F(g) = \text{Prob}(\text{gradient} \leq g) = \left(\frac{g}{g_{max}}\right)^b \quad 0 \leq g \leq g_{max} \quad (14)$$

with the exponent b related to the mean gradient $\bar{g}$ by

$$b = \frac{\bar{g}}{g_{max} - \bar{g}}. \quad (15)$$

The distribution function of storage capacity may be derived and can be shown to take the Pareto distribution form

$$F(c) = 1 - \left(1 - \frac{c}{c_{max}}\right)^b \quad c \leq c_{max}, \quad (16)$$

with the exponent b given by (15). Using (12), it then follows that the total water in storage, S(t), and the critical capacity, $C^*(t)$, are related by

$$S(t) = \frac{c_{max}}{b+1}\left[1 - \left(1 - \frac{C^*(t)}{c_{max}}\right)^{b+1}\right] \quad (17)$$

and the maximum possible total water storage for the grid square is given by

$$S_{max} = \frac{c_{max}}{b+1}. \quad (18)$$

This is also the mean store capacity, $\bar{c}$.

This storage distribution is incorporated into the Grid Model as a variant in place of the simple single storage form of the basic model. Figure 5 shows how the distribution function is used in the model to calculate the volume of direct runoff, $V(t + \Delta t)$, and the change in total water storage over the grid square, $\Delta S(t + \Delta t)$, resulting from the net water addition to storage (rainfall, less evaporation and drainage) occurring at a rate Π_i over the ith time interval $(t, t + \Delta t)$.

Topographic index formulation of soil saturation

Beven and Kirkby (1979) introduced the topographic index, $\ln(a/g)$, as a simple measure of the saturation potential at any point in the catchment, where a is the upstream area contributing to the flow at that point and g is the local surface gradient. Beven and Wood (1983) used the distribution function of topographic index to calculate

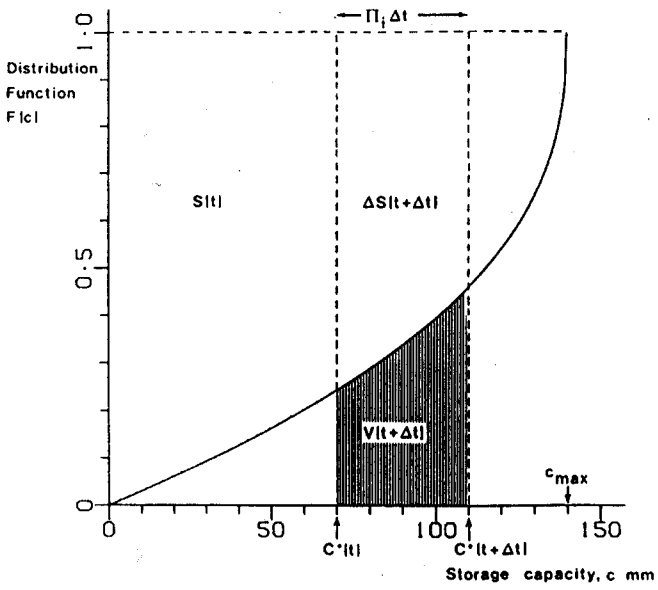

Fig. 5. *The storage capacity distribution function used to calculate the volume of direct runoff and the change in total water storage over the grid square.*

the saturation deficit at any point and the proportion of the catchment that generates runoff contributing to the fast response. Two assumptions were made. The first is that at any point in the catchment, the flow per unit width, q, is given by the exponential storage deficit function

$$q = Tg \exp(-D/m) \tag{19}$$

where D is the soil moisture deficit at that point, T is the local soil transmissivity at saturation and m is a parameter. Secondly, at any point the quantity q is proportional to the upslope contributing area, a, so

$$q = Ra \tag{20}$$

where R is a proportionality factor. Combining (19) and (20) results in the following equation for soil moisture deficit:

$$D = -m\ln(aR/Tg). \tag{21}$$

The saturated area consists of those points for which $D < 0$; that is, points for which

$$a/g < T/R. \tag{22}$$

For a given grid square of area A the average soil moisture deficit is given by

$$\bar{D} = A^{-1}\int_0^A D d\alpha = A^{-1}\int_0^A -m\ln(AR/Tg)d\alpha. \tag{23}$$

Assuming a homogeneous soil of uniform depth, so T and m are constant, then

$$\bar{D} = -m\lambda - m\ln(R/T) \tag{24}$$

where λ is a topographic constant given by

$$\lambda = A^{-1}\int_0^A \ln(a/g)d\alpha. \tag{25}$$

Since from Eqn. (21)

$$-m\ln(R/T) = D + m\ln(a/g)$$

it follows that R and T can be eliminated to give

$$\bar{D} = -m\lambda + D + m\ln(a/g). \tag{26}$$

This expression relates the average soil moisture deficit $\bar{D}$ over the grid square with topographic constant λ, to the deficit value D at a point draining an area a and having a local gradient g. The point is saturated if $D < 0$ which implies the condition

$$\ln(a/g) > \bar{D}/m + \lambda. \tag{27}$$

Use of the DTM to define topographic functions

The topographic constant λ for a grid square, given by Eqn. (25), can be readily calculated from the DTM using the approximation

$$\lambda = n^{-1}\sum_{i=1}^{n}\ln(a_i/g_i) \tag{28}$$

where n is the number of DTM points in the square.

The proportion of the square that is saturated is given by that fraction of the points for which the topographic index $\ln(a/g)$ exceeds $\bar{D}/m + \lambda$. If the fractile which is exceeded with probability ϕ is denoted as $Z(\phi)$ then the function Z is referred to as the inverse survival function. This means that if the topographic index is considered as a random variate X with distribution function $\text{Prob}(X'' x) = F(x)$ and survival function $\text{Prob}(X > x) = 1 - F(x) = S(x)$ then the inverse survival function (of probability ϕ) $Z(\phi)$ is the fractile that is exceeded with probability ϕ; that is $\text{Prob}(X > x) = \phi$ where $x = Z(\phi) = Z(S(x))$. It is the inverse survival function of the topographic index that Beven and coworkers commonly refer to as the distribution function of topographic index and display in figures.

For a given value of $\bar{D}/m + \lambda$ for a grid square the inverse survival function can be used to obtain the probability of its exceedence within the square, equivalent to the proportion of the square which is saturated. Figure 6 maps the topographic index for the Mole catchment along with the inverse survival function of topographic index, by way of illustration.

In practice the inverse survival function is approximated in the topographic index variant of the Grid Model as a four point function defined for the exceedence probabilities 0.2, 0.4, 0.6 and 0.8 corresponding to fractile values of x_1, x_2, x_3 and x_4 for the quantity $\bar{D}/m + \lambda$. If the value for $\bar{D}/m + \lambda$ lies between x_n and x_{n+1} then the saturated contributing fraction of the square is taken to be $0.2n + 0.1$; for example, if it lies between x_1 and x_2 then the fraction is 0.3. The experience of Beven (personal communication)

(a) Map of topographic index

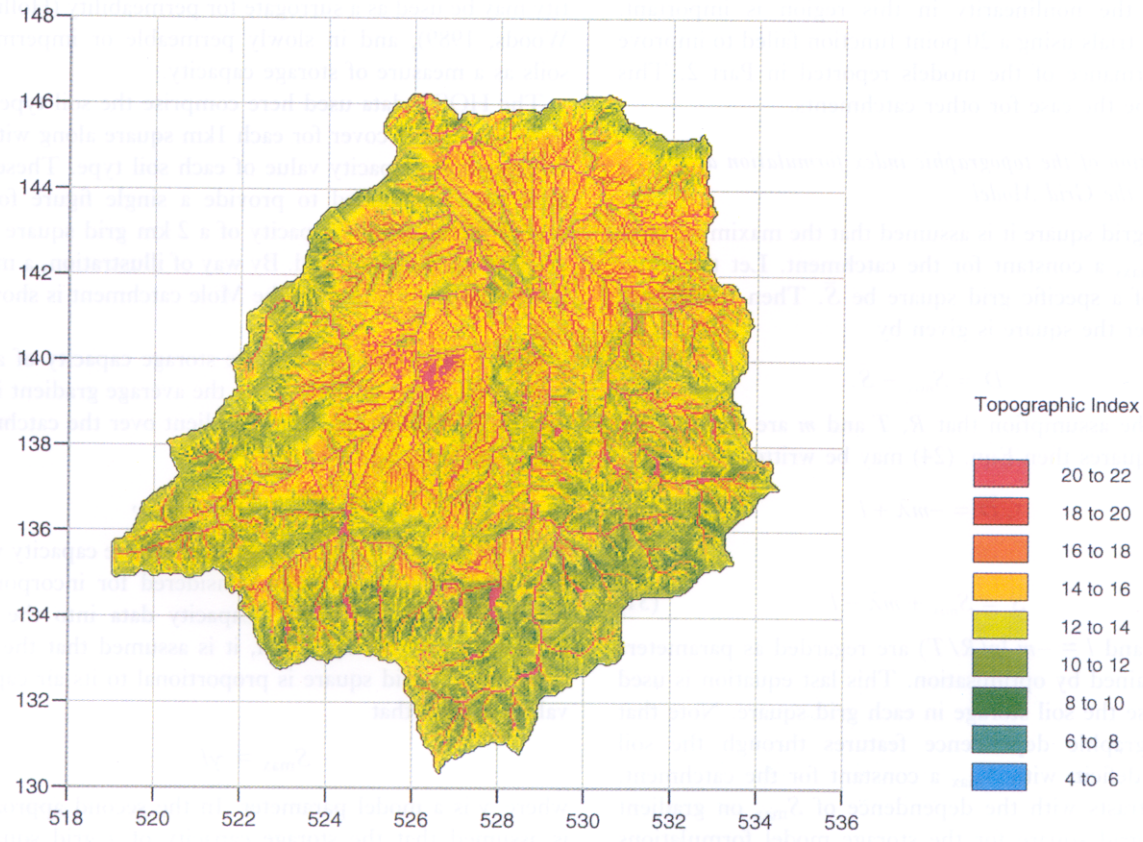

(b) Inverse survival function of topographic index

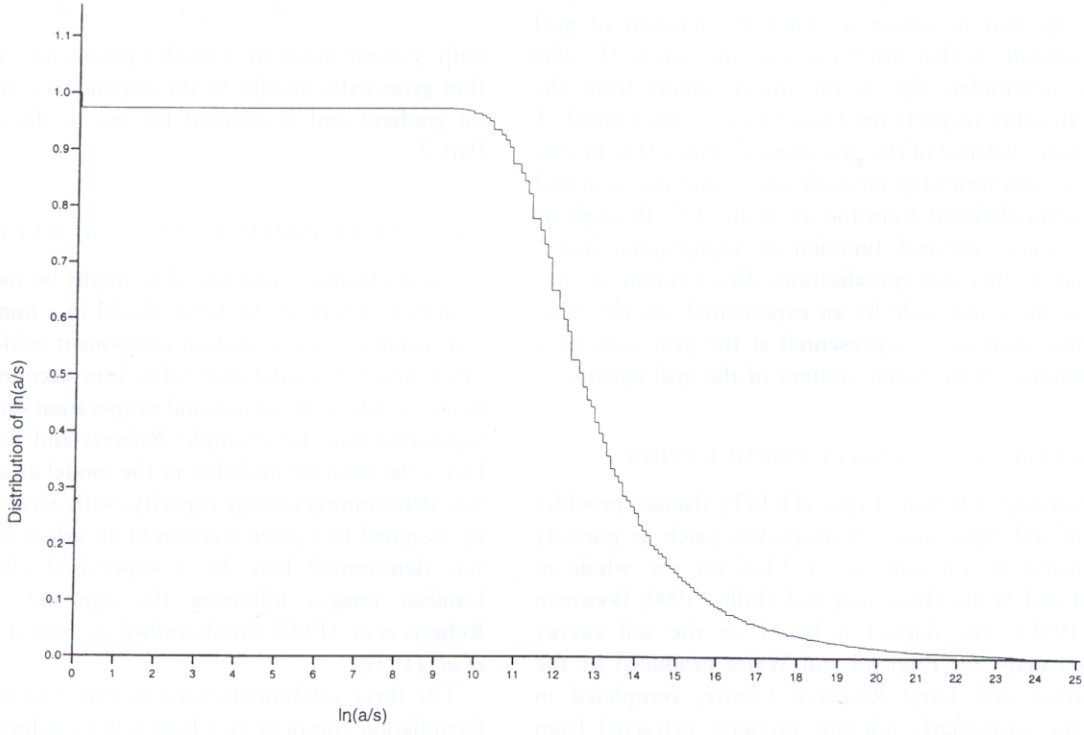

Fig. 6. *Map of topographic index and its inverse survival function for the Mole catchment.*

suggests that the nonlinear part of the function, below a relative contributing area of 0.2, is often all that is used and that the nonlinearity in this region is important. However, trials using a 20 point function failed to improve the performance of the models reported in Part 2. This may not be the case for other catchments.

Incorporation of the topographic index formulation as a variant of the Grid Model

For each grid square it is assumed that the maximum storage is S_{max}, a constant for the catchment. Let the water content of a specific grid square be $\bar{S}$. Then the storage deficit over the square is given by

$$\bar{D} = S_{max} - \bar{S}. \tag{29}$$

Making the assumption that R, T and m are constant for all grid squares then Eqn. (24) may be written as

$$\bar{D} = -m\lambda + l \tag{30}$$

so that

$$\bar{S} = S_{max} + m\lambda - l \tag{31}$$

where m and $l = -m \ln(R/T)$ are regarded as parameters to be obtained by optimisation. This last equation is used to initialise the soil storage in each grid square. Note that the topographic dependence features through the soil moisture deficit, with S_{max} a constant for the catchment. This contrasts with the dependence of S_{max} on gradient within a grid square for the storage model formulations considered previously.

The four point inverse survival function, derived from the DTM for the grid square, is used to obtain the proportion, ϕ, that is saturated. Then the amount of grid square rainfall, p, that infiltrates into the soil is $(1 - \phi)p$ and the remainder, ϕp, is the direct runoff from the square. In other respects the Grid Model is unchanged. A simple water balance of the grid storage allows $\bar{D}$ to be calculated at each time step for each square and the saturated area fraction obtained from the inequality (27) through its related inverse survival function of topographic index. Note that in this conceptualisation, direct runoff is controlled at the point scale by an exponential storage function whilst drainage is represented at the grid scale by a cubic function of the water content of the grid square.

INTEGRATED AIR CAPACITY FORMULATION

The Hydrology Of Soil Types (HOST) dataset provides details of soil types and soil properties (such as porosity and density) at a resolution of 1 km for the whole of England and Wales (Boorman and Hollis, 1990; Boorman *et al.*, 1991). The dataset is based on the soil survey 1:250,000 maps for England and Wales produced by the Soil Survey and Land Research Centre, completed in 1983. One particularly relevant property extracted from the soil survey maps is the Integrated Air Capacity of the soil layer, defined as the 'average percentage air volume over a depth of one metre'. In permeable soils, this quantity may be used as a surrogate for permeability (Hollis and Woods, 1989), and in slowly permeable or impermeable soils as a measure of storage capacity.

The HOST data used here comprise the soil types and their percentage cover for each 1km square along with the integrated air capacity value of each soil type. These data have been aggregated to provide a single figure for the overall integrated air capacity of a 2 km grid square coincident with the radar grid. By way of illustration, a map of integrated air capacity for the Mole catchment is shown in Fig. 7.

In the basic Grid Model, the storage capacity of a grid square, S_{max}, is calculated from the average gradient in the square, $\bar{g}$, and the maximum gradient over the catchment, g_{max}, via the equation

$$S_{max} = (1 - \bar{g}/g_{max})c_{max}, \tag{32}$$

where c_{max} is the regional maximum storage capacity value. Two approaches have been considered for incorporating the HOST Integrated Air Capacity data into the Grid Model. In the first approach, it is assumed that the store capacity of a grid square is proportional to its air capacity value, I, such that

$$S_{max} = \gamma I \tag{33}$$

where γ is a model parameter. In the second approach it is assumed that the storage capacity of a grid square is dependent on both the average gradient within the square and its integrated air capacity, such that

$$S_{max} = \gamma(1 - \bar{g}/g_{max})I \tag{34}$$

with γ again denoting a model parameter. This formulation gives extra weight to the dependence of soil capacity on gradient and is adopted for use in the assessment of Part 2.

LANDSAT CLASSIFIED LAND USE DATA

Landsat classified land use data might be incorporated as a further variant of the Grid Model in a number of ways. For instance, an evaporation component could be incorporated into the model that takes into account the dependence of interception loss and evaporation on land use and vegetation (see, for example, Roberts and Roberts, 1992). Here, the data are included in the model as simple indicators determining storage capacity, with zero storage capacity assigned to a given fraction of an urban area. Land use was determined here by a supervised classification of Landsat images following the approach described in Roberts *et al.* (1992) and described in more detail in Moore *et al.* (1994).

The three catchments used in Part 2 to test the model formulation comprise two high relief catchments in South Wales (the Rhondda to Trehafod) and north-west England

(the Wyre to St. Michaels), and a predominantly urban catchment in the Thames Basin (the Mole to Kinnersley Manor). The DTM was coupled with Landsat data for each catchment to produce a grid of values to represent the proportion of each grid square that is urbanised. For the high relief catchments, grid proportions were calculated as before by keeping a count of the number of DTM points classified as urban in each grid square, and dividing by the total number of DTM points in each square. For the Thames Basin, where urban areas are subdivided into percentage imperviousness classes, these values were averaged to provide a value of imperviousness for each grid square. These are then available to be used as input to the model. Initially 0.7 of the area categorised as urban was taken to have zero storage capacity (i.e. impervious). Further investigation suggested that a value nearer 0.3 might be more appropriate for Landsat classified urban areas and this factor was subsequently applied to the catchments in northwest England and Wales. Analysis of the Thames Basin imperviousness data suggests that the most common classes were 25% and 50% impervious. Figure 8 maps the impervious classes and Table 1 gives the percentage coverage for the Mole catchment by way of example. The mean value of imperviousness calculated from these data is 53% which is higher than the value of 30% suggested earlier. This may be because of the small number of categories used for the classification pushing the overall value upwards. The nature of the urban development will of course exert an influence on the impervious fraction from place to place.

Table 1. Percentage of Landsat classified urban area in each imperviousness class for the Mole catchment

Percentage impervious class	Percentage of urban area in class
100	21
75	16
50	24
25	31
0	8

Digital terrain data and velocity model variants

INTRODUCTION

The use of digital terrain data has featured prominently in the formulation of the basic Grid Model and its variants discussed previously. Further details will now be given of the DTM available for the UK and how it has been used to support model configuration and parameterisation.

A digital terrain model provides a three dimensional representation of basin topography and is configured on a large regular grid with elevation data at each grid point. The IH Digital Terrain Model used here consists of five data types derived from 1:50000 Ordnance Survey source maps. The data values for each type are located at 50 metre grid intervals, giving 400 grid points per square kilometre. The five data types are:

(i) *Ground elevation* in units of 0.1 m;
(ii) *Surface type,* whether land, river, lake or sea;
(iii) *Inflow drainage direction*, indicating which of a point's eight near neighbours drain into it. (It is not possible for all eight to flow into the same point.);
(iv) *Outflow drainage direction.* Each point is allowed to drain in only one direction determined by the overland slope;
(v) *Cumulative Catchment Area* expressed as the number of grid points that drain to a point, including that point itself.

Further details of the DTM and its derivation are given by Moore *et al.* (1994).

USE OF THE DTM TO SUPPORT MODEL FORMULATION

In the basic form of the Grid Model, the DTM is employed to supply a large dataset for each catchment using software called the Catchment Definition algorithm. The dataset contains, for each 2 km (radar) square, data relating to gradient, isochrones and the proportion of each square that lies in the catchment. The DTM and algorithm are also used to supply various parameters such as catchment area, maximum gradient and the length of unit hydrograph base (as estimated from isochrones by the maximum time-of-travel to the basin outlet).

Here, gradient is the slope of the land at that point calculated as

$$g = \tan\theta = \frac{y}{\sqrt{(y^2 + d^2)}} \tag{35}$$

where y is the change in elevation between the point and the point it flows into (the path between points can be any one of 8) and d is the plan distance between the point and the point it flows into (for the 50m DTM this is either 50 or 71 m).

Travel time, τ, is calculated by keeping track of distances covered by land and river flow paths from a point to the outlet, assuming velocities for each and calculating the travel time to the outlet from

$$\tau = \frac{\ell_L}{v_L} + \frac{\ell_R}{v_R} \tag{36}$$

where ℓ_L and ℓ_R are the distances travelled over land and river paths and v_L and v_R are the corresponding velocities.

Initial sets of isochrones were derived for the study catchments based on constant velocities of 0.5 and 0.1 m s^{-1}

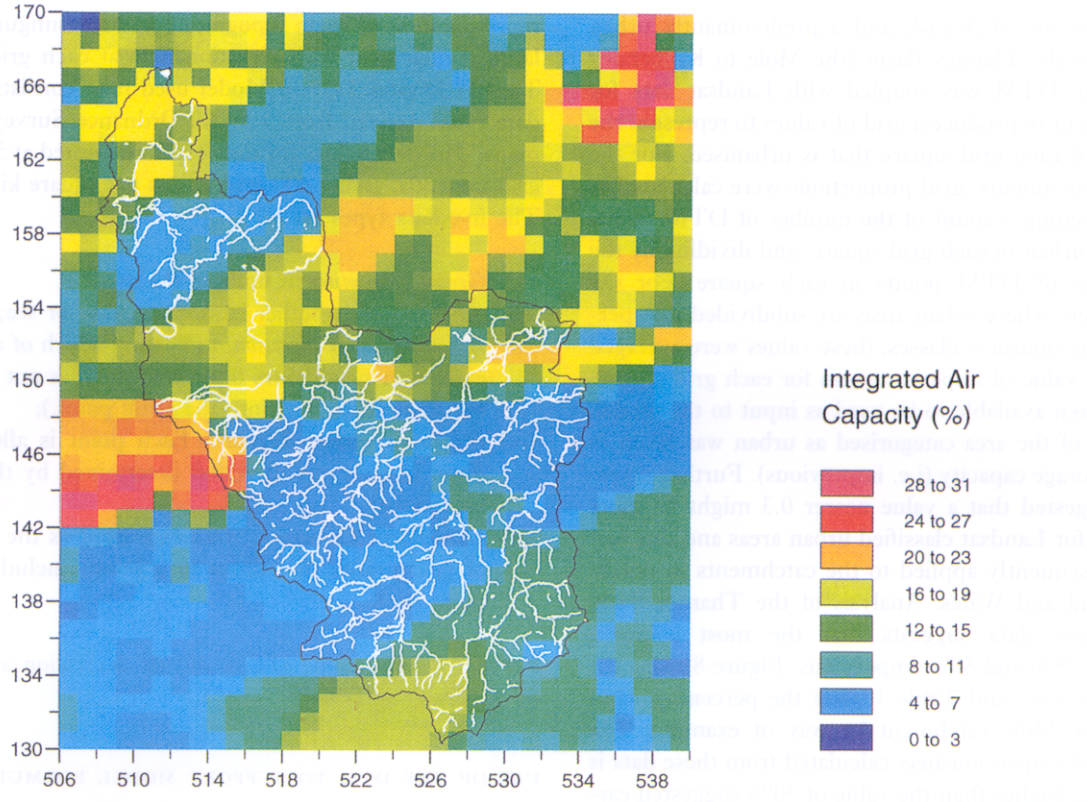

Fig. 7. *Map of integrated air capacity for the Mole catchment (to Esher).*

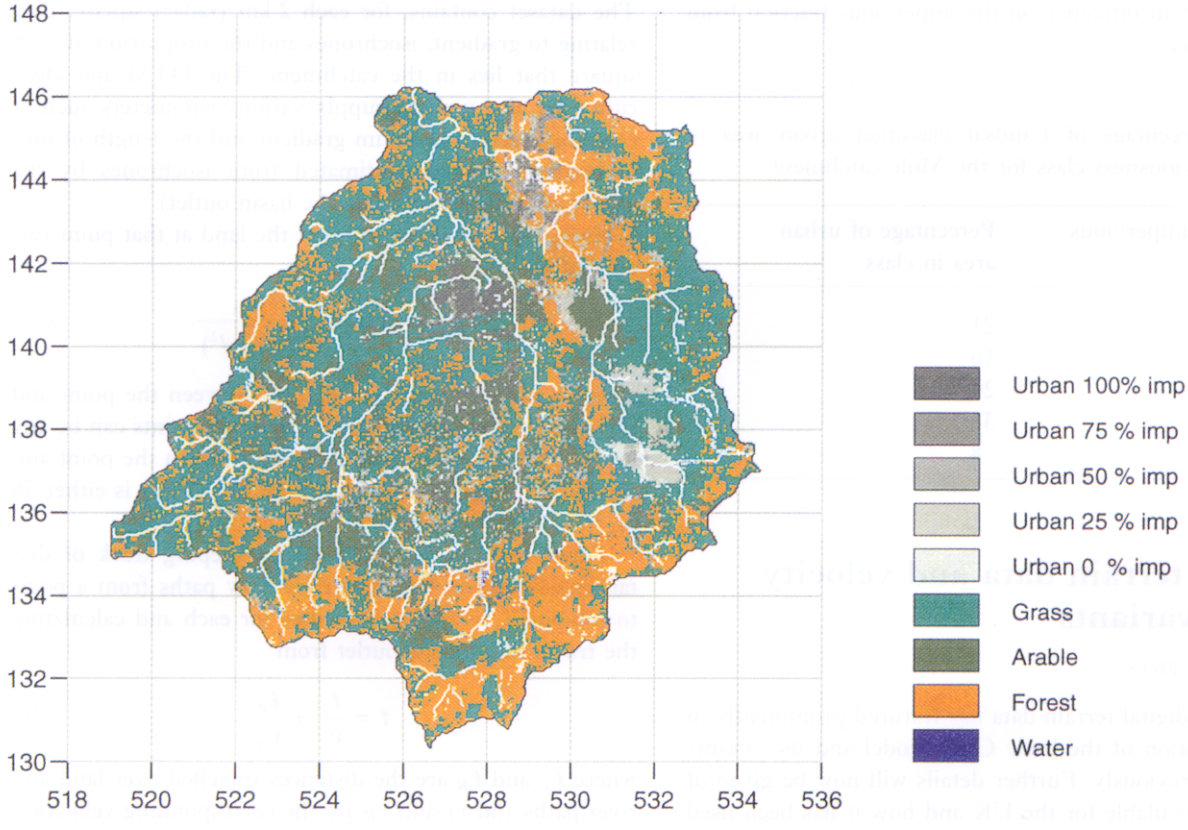

Fig. 8. *Landsat classified land use, including impervious classes, for the Mole catchment.*

for river and land paths respectively. The inferred unit hydrographs, maps of relief, gradient and the river networks, and histograms of gradient frequency within whole basins or individual radar grid squares are reproduced in Moore *et al.* (1994).

VELOCITY MODEL VARIANTS

Simple isochrones

Isochrones may be inferred from the DTM by relating velocities to morphological parameters such as gradient and stream length. The simplest approach is to assume time-of-travel, τ, to be directly proportional to stream length, ℓ, such that

$$\tau = \frac{\ell}{v} \tag{37}$$

where v is a constant representing velocity. The temporal spacing of the isochrones is taken to correspond to the model time-step, which here is 15 minutes, the same as the data time-step.

Tracer studies of variations in in-channel velocity through catchments (Pilgrim, 1977; Calkins and Dunne, 1970) suggest that average velocity remains fairly constant, or increases slightly in the downstream direction. This is consistent with data reviewed in Leopold *et al.* (1964) concerning the variation in hydraulic characteristics in channels which show that most rivers increase in velocity (slightly), depth and width in the downstream direction. The effect of a decrease in gradient would appear to be more than compensated for by increases in depth and hydraulic radius with increasing distance downstream. A model variant that employs the Chezy-Manning equation to introduce dependence on channel gradient in the calculation of velocity was investigated. However, with the introduction of the approximation of constant roughness and hydraulic radius of channels within the catchment, it can be shown that velocity is proportional to the square root of gradient, resulting in a longitudinal profile of velocity inconsistent with the slight increase in velocity in a downstream direction generally observed. Also, the gradient dependent isochrones so derived failed to improve model performance, supporting the finding of Pilgrim (1977). This variant will not be discussed further here.

Velocity variations in land flow paths are harder to quantify than for channels due to the different modes of travel taken by water across land, such as surface runoff, interflow and baseflow. Emmet (1978) presents results of laboratory experiments which suggest that the velocity of surface flow, like channel flow, increases in a downslope direction, with the effects of gradient compensated for by the retarding effects of friction on steeper gradients. However, Newson and Harrison (1978) from field studies in Plynlimon (in upland Britain) find faster velocities upstream at high flows and slower ones for lower flows. As a first approximation, the assumption of constant velocity for flow paths across land would seem reasonable.

As a starting position, isochrones were constructed assuming that time-of-travel across land and river paths is directly proportional to the path length, and the respective velocities are 0.5 and 0.1 m s^{-1}. The table below shows the unit hydrograph (UH) time-base duration in hours derived from the DTM using these velocities along with those derived from a classical unit hydrograph analysis. Note that the UHs here derive only from the isochrone formulation and do not incorporate the additional diffusive effect of the discrete kinematic routing.

	UH time base, hr	
Catchment	UH derived	DTM derived
Wyre	23	29
Mole	–	22
Rhondda	18	18

An example isochrone map for the Mole catchment is shown in Fig. 9; isochrones at an hourly time-step are presented for the sake of clarity of presentation. Figure 10 shows an example of the flow paths derived from the DTM used to obtain the isochrones, for a part of the Mole catchment.

Separate slow response pathway isochrones

A possible criticism of the basic Grid Model formulation is that both the fast and slow ('baseflow') response routing pathways are represented by isochrones whose derivation is based upon land and river velocities. To overcome this, a model variant has been introduced where the slow response routing component is based upon a second set of isochrones derived from a consideration of the Darcy velocity of flow through a porous medium, $Kdh/d\ell$, where K is the hydraulic conductivity (permeability), h is the piezometric head and ℓ is the thickness of the medium.

The wave velocity required here has been approximated by

$$v = kg, \tag{38}$$

where g is the local gradient of the terrain as estimated from the DTM and k is a parameter which allows optimisation of the slow response isochrones. Time-of-travel of every point in the catchment to the outlet is then calculated from

$$t_i = \frac{1}{k}\sum_i \frac{d_i}{g_i} \tag{39}$$

where d_i is the distance between the ith and the $(i-1)$th points on the flow path, g_i is the gradient between the points and k is the parameter found by calibration.

Isochrone optimisation

A natural extension of the fixed velocity model is to incorporate the determination of the fixed velocity values into

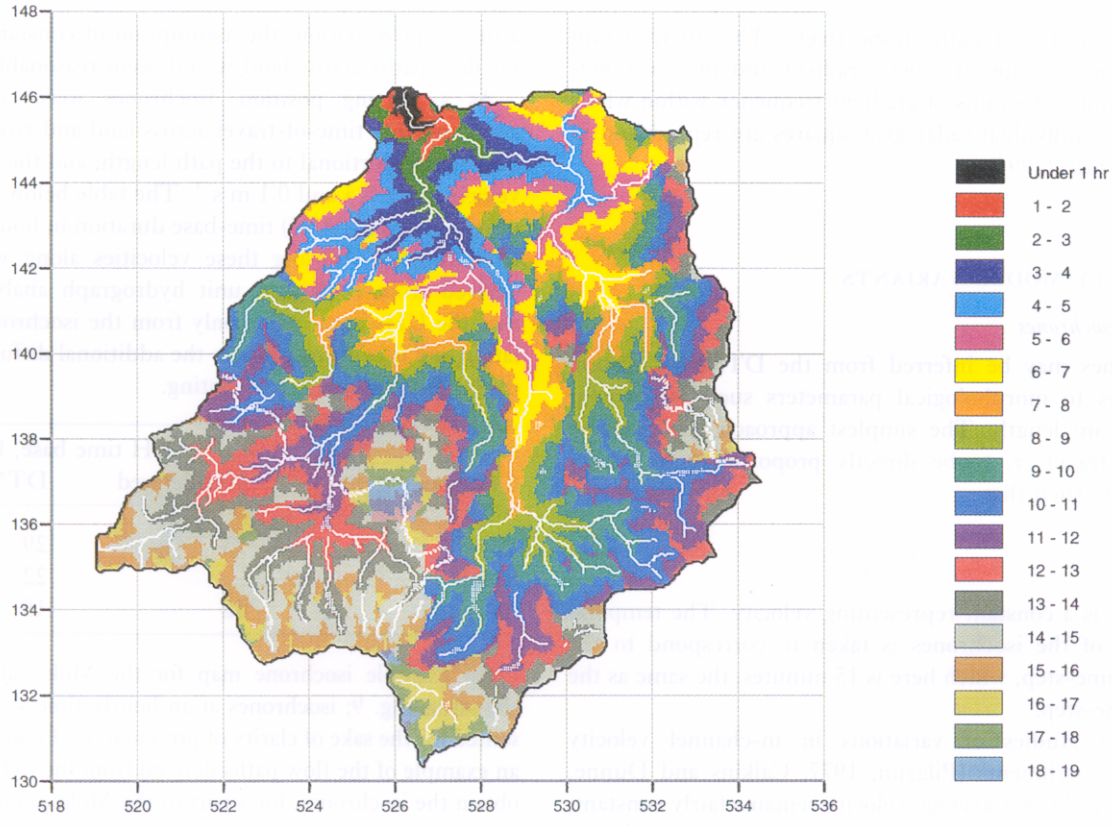

Fig. 9. *Isochrone map for the Mole catchment.*

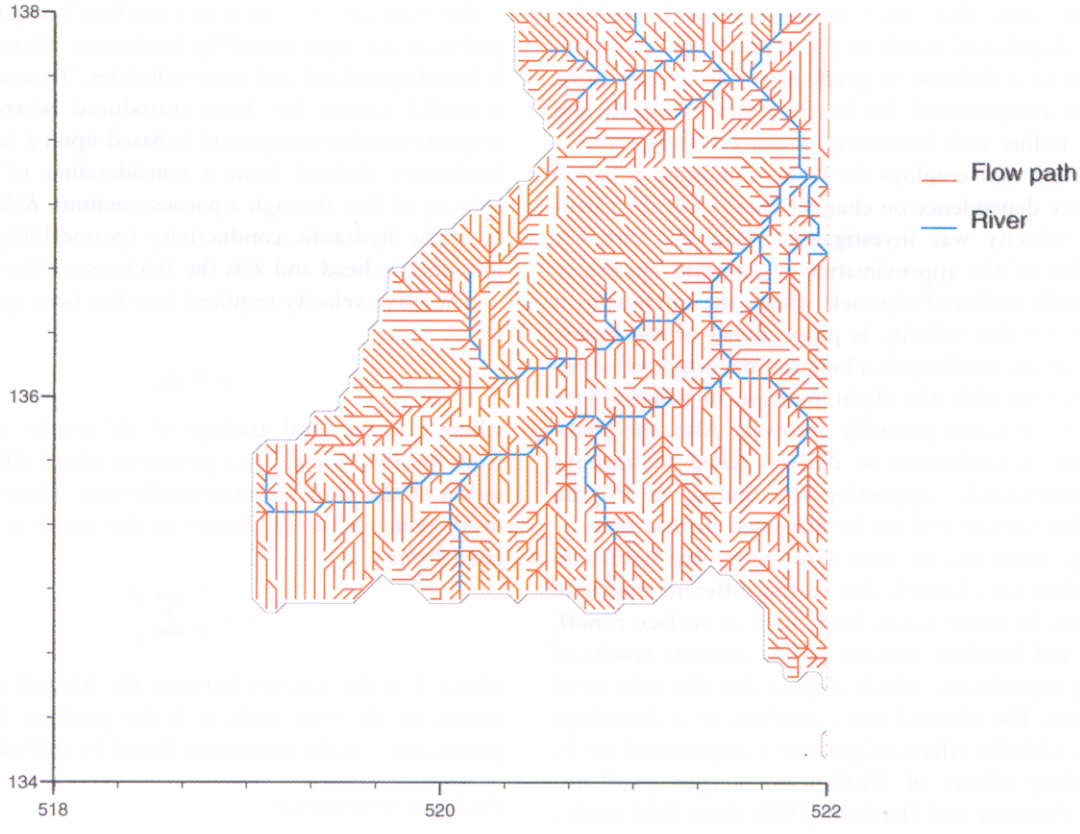

Fig. 10. *DTM-derived flow paths for part of the Mole catchment.*

the model optimisation framework. The Catchment Definition algorithm, employed to extract information from the DTM for use by the model, was adapted to produce sufficient information for the model to update the grid-isochrone area fractions, w_{ij}, as velocities are changed during parameter optimisation. For each DTM point in the catchment, the minimum information necessary to calculate the new isochrones consists of j, the number of the model grid square, and ℓ_L and ℓ_R, the distances travelled over land and river to the DTM point. Land and river velocities are regarded as model parameters, with travel times of each grid point to the outlet calculated as previously, using Eqn. (36).

Optimisation of the isochrone velocities proved successful in improving the accuracy of model simulations. In general, optimisation has the effect of increasing the river velocity and decreasing the land velocity from the base values of 0.5 and 0.1 m s^{-1} respectively, and usually gives a longer unit hydrograph base.

SUMMARY

A Catchment Definition algorithm has been developed to derive, from a DTM, data on gradient and path length along with the proportion of each grid square that lies in the catchment. These data can be transferred to the Grid Model, and used as part of a calibration procedure to estimate land and river velocities and, using path length, to derive a set of optimal isochrones for the catchment. The set of isochrone bands determine the spatial discretisation of the discrete kinematic routing procedure. Each band is represented by a routing reach characterised by a dimensionless wave speed parameter, further controlling the attenuation of a flood wave. The basic form of Grid Model employs the same set of isochrones for fast and slow response pathways in a parallel configuration, but with different wave speeds θ_s and θ_b respectively. A variant, motivated by a consideration of Darcy flow in a porous medium, allows velocity to vary with the local terrain gradient from which separate slow response ('baseflow') isochrones are calculated. The routing cascade configured on this isochrone band spacing receives drainage from the grid storages as input, whilst the fast response routing cascade receives direct runoff from the grid storages as input. Summing the routed flows from the fast and slow pathways gives the total basin runoff.

Parameterisation of the Grid Model and its variants

Table 2 lists the set of parameters used by the IH Grid Model, including its variants. Although 14 parameters are listed, some relate only to specific variants and are not all used at any one time. Also, many of them are not used in the calibration process and simply take recommended values. The infiltration excess mechanism of Eqn. (4) is considered unnecessary in the basins considered here, so

Table 2. Model parameter descriptions and units

Symbol	Description of parameter	Units
f_r	Rainfall correction factor	—
D*	Storage threshold deficit (or root constant) in evaporation function	mm
S_0	Proportion of total storage capacity initially full	—
g_{max}	Regional upper limit of gradient	—
c_{max}	Regional upper limit of storage capacity	mm
i_{max}	Maximum infiltration rate	mm h^{-1}
k_d	Storage constant of (cubic) drainage function	h^{-1} mm^{-2}
θ_s	Wave speed parameter for routing direct runoff	—
θ_b	Wave speed parameter for routing drainage	—
v_L	Advection velocity of flow along land path	m s^{-1}
v_R	Advection velocity of flow along river path	m s^{-1}
Darcy slow response isochrone variant		
k	Darcy velocity parameter, analagous to hydraulic conductivity	m s^{-1}
Topographic index variant		
m	Parameter in exponential storage deficit function	mm
l	$l = -m \ln (R/T)$ introduced in Eqn. (31)	mm
IAC variant		
γ	Factor of proportionality between IAC and store capacity	mm

the maximum infiltration rate, i_{max}, was set to an artificially high value. The storage threshold deficit controlling evaporation was also kept constant at 40mm.

The parameters that are usually calibrated are: the advection velocities v_R and v_L of the flow along river and land paths respectively, which determine the isochrone pathways; the wave speed parameters for kinematic routing of slow and fast response flows, θ_b and θ_s; the storage constant, k_d, of the cubic drainage function in Eqn. (3); and the rainfall correction factor, f_r, used as a constant multiplicative factor to overcome any deficiencies in the rainfall measurements, from radar and/or raingauges. The rainfall correction factor is initially set to 1, unless there is clear evidence to the contrary, and adjusted only at a secondary stage of calibration in order not to distort the overall calibration unduly.

Values of g_{max} and c_{max} are the regional upper limits of gradient and storage capacity. They are set initially to the catchment values, obtained as the maximum of the grid mean values as calculated from the DTM, and increased to optimal 'regional' values as part of the model calibration procedure. The parameter S_0 is the initial total water storage content fraction, used to initialise the stores with respect to antecedent precipitation. If the topographic index model variant is invoked, gradient data for each grid square are no longer needed. Instead, values for the topographic constant, λ, given by Eqn. (28) are derived from the DTM and used by the model. The two parameters g_{max} and S_0 are replaced by the two topographic parameters used in Eqn. (31) to initialise the soil moisture store in each grid square, namely m and $l = -m\ln(R/T)$. Finally, the integrated air capacity model variant uses an additional dataset of air capacity data, together with a new parameter, γ, used in Eqns. (33) or (34), which replaces c_{max}, the regional upper limit of storage capacity. The drainage exponent β in Eqn. (3) is here regarded as a constant equal to 3 and therefore not included in Table 2; for other applications it might be considered as a parameter to be optimised.

To summarise, the basic model has five main parameters that are always used in model calibration, the routing parameters v_L, v_R, θ_s and θ_b together with the drainage parameter k_d. Also used is the initialisation parameter for the total water in storage fraction, S_0, and the rainfall correction factor, f_r, if necessary. The regional parameters controlling runoff production, g_{max} and c_{max}, can be estimated using DTM gradient data and knowledge of the local soils and geology, or by calibration to give the best model fit.

Summary and conclusions

A practical methodology for distributed rainfall-runoff modelling suitable for use with grid square radar data has been developed. The basic form of model, referred to as the Simple Grid Model or SGM, is based on two fundamental model components. The first is a runoff production function which controls the generation of flood runoff within a grid square area and the second is a routing function which represents the translation of water through the catchment to its outlet. The runoff production function is based on the concept that a given grid square has a certain capacity to absorb water. This 'storage capacity' is assumed to vary as a function of topographic gradient, steeper slopes having a smaller capacity to absorb water. The problem of over-parameterisation has been circumvented through the use of measurements from a contour map or digital terrain model of the basin together with simple linkage functions. These functions allow many model variables to be prescribed through a small number of regional parameters which can be optimised to obtain a good model fit. Using the DTM to measure the average gradient within a grid square it is possible to infer the storage capacity of every grid square making up the catchment using a simple linkage function relating capacity to gradient. This function is defined through only two regional parameters, g_{max} and c_{max}, denoting upper limits of gradient and storage capacity respectively. Further parameters are introduced to allow for drainage to 'groundwater' and to represent evaporation loss as a function of water storage deficit.

The routing function is based on the classical isochrone concept in which the time-of-travel to the basin outlet is related directly to the length of the flow path from the point of interest to the outlet. In practice, two routing cascades are used, one to carry saturation excess runoff and the other drainage from the grid stores. These may be equated to channel and groundwater pathways for convenience.

A number of variants on the SGM have been considered including a continuous parametric representation of variability in storage capacity, called the Probability-distributed Grid Model or PGM. In this model the variation of gradient within a grid square is represented by a probability density function which, through the gradient-capacity linkage function, is used to derive the distribution of storage capacity within the square. A formulation based on the power distribution of gradient has been developed which gives a Pareto distribution of storage capacity. A further variant is explored based on a topographic index measure of saturation potential, defined by contributing area in addition to gradient. When used in combination with an exponential storage deficit function, it provides a basis for determining the saturation excess runoff and water balance of a grid square. It is shown that the proportion of the grid square which is saturation is given by the inverse survival function of the topographic index, evaluated at a critical threshold value which depends on the average values of soil moisture deficit and topographic index for the square.

An evaluation of the performance of the SGM and its variants is presented in Part 2 (Bell and Moore, 1998).

Here, the distributed model variants are assessed on three catchments in the UK in both simulation and updating mode, and judged for their suitability for use in real-time flood forecasting with reference to a lumped model used operationally.

Acknowledgements

This research has been supported by the National Rivers Authority (now part of the UK Environment Agency), the Ministry of Agriculture, Fisheries and Food under its Flood and Coastal Defence Commission and the Commission of the European Communities under the EPOCH Project 'Weather Radar and Storm and Flood Hazard' and the Environment Programme Project 'Storms, Floods and Radar Hydrology'. Particular thanks are due to George Merrick of the Environment Agency for his role as project co-ordinator. The referees are thanked for ideas leading to a greater clarity of presentation.

References

Anderl, B., Attmannspacher, W. and Schultz, G.A., 1976 Accuracy of reservoir inflow forecasts based on radar rainfall measurements, *Wat. Resour. Res.*, **12**, 217–223.

Bell, V.A. and Moore, R.J., 1998 A grid-based distributed flood forecasting model for use with weather radar data: Part 2. Case studies, *Hydrol. Earth System Sci.*, **2**, 283–298.

Beven, K.J. and Kirkby, M.J., 1979 A physically based, variable contributing area model of basin hydrology, *Hydrol. Sci. Bull.*, **24**, 43–69.

Beven, K.J. and Wood, E.F., 1983 Catchment geomorphology and the dynamics of runoff contributing areas, *J. Hydrol.*, **65**, 139–158.

Boorman, D.B. and Hollis, J.M., 1990 Hydrology of Soil Types. A hydrologically-based classification of the soils of England and Wales. *MAFF Conference of River and Coastal Engineers*, Loughborough, UK, Ministry of Agriculture, Fisheries and Food, 8pp.

Boorman, D.B., Hollis, J. and Lilly, A., 1991 The production of the Hydrology Of Soil Types (HOST) data set. *BHS 3rd National Symp.*, Southampton, 6.7–6.13, British Hydrological Society.

Calkins, D., and Dunne, T., 1970 A salt tracing method for measuring channel velocities in small mountain streams, *J. Hydrol.*, **11**, 379–392.

Chander, S. and Fattorelli, S., 1991 Adaptive grid-square based geometrically distributed flood forecasting model. In: Cluckie, I. D. and Collier, C. (Eds.), *Hydrological Applications of Weather Radar*, Ellis Horwood, 424–439.

Collier, C.G., 1996 *Applications of weather radar systems: a guide to uses of radar data in meteorology and hydrology*. 2nd edn., Wiley, Chichester, UK.

Emmet, W.W., 1978 Overland Flow. In: Kirby, M. J. (ed.), *Hillslope Hydrology*. 145–175, Wiley.

Hollis, J.M. and Woods, S.M., 1989 *The measurement and estimation of soil hydraulic conductivity*. SSLRC Research Report for MAFF Project c(i), Soil Survey and Land Research Centre, 25pp.

Leopold, L.B., Wolman, M.G., and Miller, J.P., 1964 *Fluvial Processes in Geomorphology*. W. H. Freeman, San Francisco.

Moore, R.J., 1985 The probability-distributed principle and runoff prediction at point and basin scales, *Hydrol. Sci. J.*, **30**, 273–297.

Moore, R.J., 1991 Use of meteorological data and information in hydrological forecasting. In: A. Price-Budgen (Ed.), *Using Meteorological Information and Products*, 377–396, Ellis Horwood.

Moore, R.J., 1992 Grid-square rainfall-runoff modelling for the Wyre catchment in North-West England. *Proceedings of the CEC Workshop: Urban/rural application of weather radar for flow forecasting*, 3–4 December 1990, Dept. of Hydrology, Soil Physics and Hydraulics, University of Wageningen, The Netherlands, 4pp.

Moore, R.J. and Bell, V.A., 1996 A grid-based flood forecasting model using weather radar, digital terrain and Landsat data, *Quaderni Di Idronomia Montana*, **16**, (Special Issue, Proc. Workshop on 'Integrating Radar Estimates of Rainfall in Real-Time Flood Forecasting'), 97–105.

Moore, R.J. and Jones, D.A., 1978 An adaptive finite-difference approach to real-time channel flow routing. In: Vansteenkiste, G.C. (ed.), *Modelling, Identification and Control in Environmental Systems*, North Holland.

Moore, R.J. and Bell, V., 1994 A grid square runoff model for use with weather radar data. In: M.E. Almeida-Teixeira, R. Fantechi, R. Moore and V.M. Silva (eds), *Advances in Radar Hydrology*, Proc. Int. Workshop, Lisbon, Portugal, 11–13 November 1991, European Commission, Report EUR 14334 EN, 303–311.

Moore, R.J., Bell, V., Roberts, G.A. and Morris, D.G., 1994 *Development of distributed flood forecasting models using weather radar and digital terrain data.* R&D Note 252, Research Contractor: Institute of Hydrology, National Rivers Authority, 144pp.

Newson, M.D. and Harrison, J.G., 1978 *Channel studies in the Plynlimon experimental catchments*. Report No 47, Institute of Hydrology, Wallingford, Oxon, UK, 61pp.

O'Connell, P.E. and Clarke, R.T., 1981 Adaptive hydrological forecasting—a review, *Hydrol. Sci. Bull.*, 26, 179–205.

Pilgrim, D.H., 1977 Isochrones of travel time and distribution of flood storage from a tracer study on a small watershed, *Wat. Resour. Res.*, **13**, 587–595.

Polarski, M., 1992 *A review of conceptual rainfall-runoff models using digitally distributed data*, Report to MAFF, Institute of Hydrology, Wallingford, Oxon, UK, 36pp.

Roberts, G.A., France, M. and Robinson, R., 1992 Computing the water balance of a small agricultural catchment in southern England by consideration of different land use types. I. Land classification using remotely-sensed imagery, *Agric. Wat. Manag.*, **21**, 145–154.

Roberts, G. and Roberts, A., 1992 Computing the water balance of a small agricultural catchment in southern England by consideration of different land use types. II. Evaporative losses from different vegetation types, *Agric. Wat. Manag.*, 21, 155–166.

Todini, E., 1988. Rainfall-runoff modelling—past, present and future, *J. Hydrol.*, **100**, 341–352.